HHS Public Access

Author manuscript

Clin Cancer Res. Author manuscript; available in PMC 2021 August 01.

Published in final edited form as:

Clin Cancer Res. 2021 February 01; 27(3): 785–798. doi:10.1158/1078-0432.CCR-20-2769.

A novel neoplastic fusion transcript, RAD51AP1-DYRK4, confers sensitivity to the MEK inhibitor trametinib in aggressive breast cancers

Chia-Chia Liu[1,2,3,*], **Jamunarani Veeraraghavan**[4,5,6,*], **Ying Tan**[4,5,6], **Jin-Ah Kim**[4,5,6], **Xian Wang**[1,2,3,4,5,6], **Suet Kee Loo**[1,2,3], **Sanghoon Lee**[1,2,3], **Yiheng Hu**[1,2,3,4,5,6], **Xiao-Song Wang**[1,2,3,4,5,6,#]

[1]UPMC Hillman Cancer Center, University of Pittsburgh, Pittsburgh, PA, 15232, USA.

[2]Department of Pathology, University of Pittsburgh, Pittsburgh, PA, 15232, USA.

[3]Department of Biomedical Informatics, University of Pittsburgh, Pittsburgh, PA, 15232, USA.

[4]Lester & Sue Smith Breast Center, Baylor College of Medicine, Houston, TX 77030, USA.

[5]Dan L. Duncan Cancer Center, Baylor College of Medicine, Houston, TX 77030, USA.

[6]Department of Medicine, Baylor College of Medicine, Houston, TX 77030, USA.

Abstract

Purpose: Luminal B breast tumors are more aggressive estrogen receptor positive breast cancers characterized by aggressive clinical behavior and a high risk of metastatic dissemination. The underlying pathological molecular events remain poorly understood with a paucity of actionable genetic drivers, which hinders the development of new treatment strategies.

Experimental Design: We performed large-scale RNAseq analysis to identify chimerical transcripts preferentially expressed in luminal B breast cancer. The lead candidate was validated by Reverse Transcription PCR in breast cancer tissues. The effects of inducible ectopic expression or genetic silencing were assessed by phenotypic assays such as MTS, transwell and transendothelial migration assays, and by clonogenic assays to assess MEK inhibitor sensitivity. Subcellular fractionation, western blots, and immunoprecipitation were performed to characterize the protein products and elucidate the engaged mechanisms.

Results: Here we report a novel tumor-specific chimeric transcript RAD51AP1-DYRK4 preferentially expressed in luminal B tumors. Analysis of 200 ER-positive breast tumors detected RAD51AP1-DYRK4 overexpression in 19 tumors (9.5%), which is markedly enriched in the

[#]**Corresponding Author**: Xiaosong Wang, M.D., Ph.D., Associate Professor of Pathology and Biomedical Informatics, UPMC Hillman Cancer Center, 5117 Centre Avenue, Research Pavilion, Room G.5a, Pittsburgh, PA 15232, Phone: 412-623-1587, xiaosongw@pitt.edu.

[*]Chia-Chia Liu and Jamunarani Veeraraghavan contributed equally to this project.

Authors contributions

C.C. L. and J.V. and designed and performed cell biology and mechanistic experiments, analyzed the data and co-wrote the manuscript. Y.T. designed and performed molecular biology experiments. J.A.K., X.W., S.K.L. and Y.H. assisted in the molecular and cell biology experiments. S.H.L. assisted in bioinformatics analysis. X-S.W. conceived and supervised the study, performed bioinformatics analysis, and wrote the manuscript.

Conflict of Interests: The authors declare no conflict of interests.

luminal B tumors (17.5%). Ectopic expression of RAD51AP1-DYRK4, but not wild-type RAD51AP1, leads to marked activation of MEK/ERK signaling, and endows increased cell motility and transendothelial migration. More importantly, RAD51AP1-DYRK4 appears to endow increased sensitivity to the MEK inhibitor Trametinib through attenuating compensatory activation of HER2/PI3K/AKT under MEK inhibition.

Conclusions: This discovery sheds light on a new area of molecular pathobiology of luminal B tumors and implies potential new therapeutic opportunities for more aggressive breast tumors overexpressing this fusion.

INTRODUCTION

Estrogen receptor positive (ER+) breast cancer, also known as luminal breast cancer, can be classified into A and B intrinsic subtypes. Luminal B breast cancer accounts for 15–20% of all breast cancers (1), and is the most common subtype in young women (2). While the luminal A tumors can be effectively treated with endocrine therapy, the luminal B tumors are characterized by higher proliferation index, more aggressive behavior, and endocrine resistance. Clinically luminal B cancers show increased early relapse rates with a metastasis time pattern similar to basal-like breast cancer, and the treatment options are limited to concomitant endocrine and chemotherapy (3). Apart from higher growth factor signaling activities (4), their underlying pathological molecular events remain ill understood. The recent transcriptome and genome sequencing studies have revealed a paucity of actionable oncogenic drivers in these tumors (5), which hinders the development of new diagnostic and treatment strategies.

In our previous study, we have identified a recurrent *ESR1-CCDC170* rearrangement in 6–8% of luminal B breast cancers which endows enhanced aggressiveness and reduced endocrine sensitivity (6). This fusion was subsequently verified by several other studies (7–10). In the present study, through a large-scale analysis of RNAseq data from The Cancer Genome Atlas (TCGA), we discovered a neoplastic chimerical transcript, *RAD51AP1-DYRK4* that is silent in almost all human normal tissues but is markedly overexpressed in 3.6–9.5% of luminal breast cancer. More importantly, the overexpression of this chimera is associated with luminal B breast cancers (7–17.5 %), and tends to be present in the tumors that are negative for *ESR1-CCDC170* rearrangements. In this study, we investigated the molecular characteristics, clinical relevance, oncogenic and therapeutic role of RAD51AP1-DYRK4 in the more aggressive form of luminal breast cancers. We discovered that RAD51AP1-DYRK4 endows enhanced activation of MEK/ERK signaling and increased aggressiveness of luminal breast cancers, and more importantly confers MEK inhibitor (MEKi) sensitivity via repressing MEKi-induced PI3K/AKT activation.

MATERIALS AND METHODS

Analyses of TCGA RNAseq data.

The RNAseq (Illumina HiSeq, paired-end) data for breast tumors used in this study were from TCGA cghub (https://cghub.ucsc.edu). Paired-end RNAseq data from TCGA for 1059 breast tumors and 111 paired normal breast tumors were aligned to human genome build 19

using the Tophat 2.0.3 fusion junction mapper, with parameters allowing for detection of fusion transcripts between adjacent genes (min distance of detected junction breakpoints = 5kb). Using our Perl script pipeline called “Fusion Zoom”, the putative fusion junctions were mapped to human exons (derived from UCSC gene and Ensemble gene) to identify authentic chimerical sequences. The putative fusion transcripts are required to be supported by a minimum of one read that maps to the exon junctions of the two fusion genes. This criterion was expected to filter out most artifactual gene fusions resulting from random ligations during the sequencing library preparation. Putative fusion sequences were then reconstructed and aligned with the human genome and transcriptome using BLAST. The chimeric sequences that can mostly align to a wild-type genomic or transcript sequence were disregarded. The tumor samples that harbor a total of three supporting reads of candidate chimeras are considered as positive cases. After such filtering, the fusion candidates that are found at least two breast tumors with no reads detected in paired adjacent normal breast tissues were identified. A total of 1206 putative fusions were identified as somatic and recurrent; their preferential presence in luminal B tumors compared to luminal A tumors was assessed based on two proportion Z-test with a cutoff of $p<0.05$. The luminal B enriched fusion candidates were then ranked by the incidence of fusion transcripts in breast tumors, their average abundance (median number of supporting reads), and the concept signature (ConSig) score (http://consig.cagenome.org, release 2) that prioritizes biologically meaningful candidate genes underlying cancer (11).

TCGA RPPA data analysis.

Reverse Phase Protein Array (RPPA) data generated based on replicate-based normalization (RBN) was extracted from The Cancer Proteome Atlas (TCPA). The RBN method uses replicate samples run across multiple batches to adjust the data for batch effects (12). For analysis, the RPPA results for MEK and ERK signaling in *RAD51AP1-DYRK4*-positive cases were compared against the fusion-negative luminal B cases overexpressing wtRAD51AP1. Statistical significance was analyzed by Student’s t-test.

Tissue collections.

All breast tumor tissues were obtained from the Tumor Bank of the Lester and Sue Smith Breast Center at Baylor College of Medicine. Total RNA for normal breast tissues (5 Donor Pool) was purchased from BioChain (R1234086-P).

RT-PCR.

RT-PCR was performed with Platinum Taq Polymerase High Fidelity (Life Technologies) and RAD51AP1-DYRK4 fusion-specific primers (Supplementary Table S4). RAD51AP1-DYRK4 PCR products from several cell lines and tumors were purified, cloned into pCR4-TOPO vectors, and sequenced. RT-PCR band intensities were quantified using ImageJ software, and the ROCR module of R statistical package was used to determine the optimal cutoff for RAD51AP1-DYRK4 or wtRAD51AP1 overexpression (Supplementary Fig. S3).

Quantitative real-time PCR.

Total RNA was extracted using RAN$_{zol}$ ® RT (Molecular Research Center Inc., Cincinnati, OH, USA) according to the manufacturer's instructions. RNA was converted to cDNA using the Transcriptor First Strand cDNA Synthesis Kit (Roche). Gene expression level were determined by SYBR Green PCR Master Mix (Applied Biosystems). Analysis was performed using QuantStudio 3 System (ThermoFisher Scientific). The qPCR primers are provided in Supplementary Table S4. Expression levels were presented relative to the GAPDH (glyceraldehyde-3-phosphate dehydrogenase) housekeeping gene.

Inducible RAD51AP1-DYRK4 expression vector and stable cell lines.

RAD51AP1-DYRK4 fusion variants containing the full-length ORFs were amplified from fusion positive cell lines HCC1187 and HCC38, using Roche Expand Long Range dNTPack. The RAD51AP1-DYRK4 fusion cDNAs were then subcloned into an inducible lentiviral pTINDLE vector provided by Dr. Xuewen Pan. After verification by sequencing, these constructs were infected into T47D cells and selected using Geneticin (Invitrogen).

Cell culture.

The major cell lines used in this study including T47D, MDA-MB361, HCC1937, HCC38, HCC1428, MCF12A and human umbilical vein endothelial cells (HUVECs) were obtained from American Type Culture Collection (ATCC). ATCC distributed cell lines are authenticated routinely through short tandem repeat (STR) profiling and are low passage and contamination free. The MCF7 cells were a kind of gift of D. Mark E. Lippman and were authenticated by MD Anderson Cell Authentication Core Facility through STR profiling. The ZR-75–30 cells were obtained from NCI-ICBP-45 human breast cancer cell line kit. 293FT cells used for lentivirus packaging were purchased from Invitrogen. Cell lines are routinely tested for mycoplasma contamination following a published protocol (13). T47D, HCC1937, MCF7, HCC38, HCC1428 and ZR75–30 cells were cultured in RPMI 1640 (Cellgro, Corning) with 10 % fetal bovine serum, and MDAMB361 cells were cultured in DMEM (Gibco, Thermo Fisher Scientific) with 20% fetal bovine serum (Hyclone, Thermo Fisher Scientific). MCF12A cells were grown in Dulbecco's Modified Eagle's/F12 medium (DMEM/F12, 1:1) containing 5% horse serum (Sigma-Aldrich), 20 ng/mL epidermal growth factor, 0.5 μg/mL hydrocortisone, 0.1 μg/mL cholera toxin, and 10 μg/mL human insulin. 293FT cells were cultured in DMEM with 10 % fetal bovine serum. HUVECs were cultured using the MEBM basal medium (CC-3151) and MEGM bullet kit (CC-3150) (Lonza).

siRNA knockdown.

The 5'RAD51AP1#1 (5'-GCCAGUGAUUAUUUAGAUU-3'), 5'RAD51AP1#2 (5'-GAACAGCACCAAAGGAGUU-3') and 3'RAD51AP1#1 (5'-CAGAUUAGCACGAGUUAAA-3'), 3'RAD51AP1#2 (5'-CUUCAAGACUUCAAUGAGAUU-3'), DYRK4#1 (5'-CUGCGAAGGUUGGAAGUAAUU −3') and DYRK4#2 (5'-AUCAAGAACUCCAGAAUGAUU-3') siRNAs were purchased from Dharmacon and transfected using Lipofectamine RNAi MAX Reagent (Invitrogen) according to manufacturer's instructions.

Western blot.

For immunoblot analysis, E9-E2 and wtRAD51AP1 expression was induced in transduced T47D cells with 200ng/ml doxycycline for one week. Total proteins were extracted by homogenizing the cells in RIPA Lysis Buffer (Sigma-Aldrich), supplemented with complete protease inhibitor cocktail tablet (Roche Diagnostics), 50mM beta-Glycerophosphate, 1mM sodium orthovanadate, 1mM sodium fluoride, and 1mM PMSF. Thirty micrograms of protein extracts were denatured in sample buffer, separated by SDS-PAGE, and transferred onto a nitrocellulose membrane (Invitrogen). The membranes were blocked and incubated overnight at 4°C with primary antibodies. The primary antibodies are provided in Supplementary Table S5. The membranes were then incubated with the respective horseradish peroxidase-conjugated secondary antibody and the signals were visualized by the enhanced chemiluminescence system (Bio-rad) as per the manufacturer's instructions. For the blots shown in Fig. 6A, the E9-E2 and wtRAD51AP1 expressing T47D cells were seeded in a 10 cm^2 dish with or without 200ng/ml doxycycline treatment and incubated for one week. After doxycycline treatment, the cells were seeded at a density of 1.5×10^6 in new 6cm^2 dishes with or without 200ng/ml doxycycline containing 0.5uM trametinib or DMSO for 24 hours and harvested cells for immunoblotting analysis.

Generating polyclonal antibody specifically detecting DYRK4 frame-shift peptide.

The polyclonal antibody specifically detecting RAD51AP1-DYRK4 was generated by GenScript Biotech, NJ. In brief, the peptide sequence of E9-E2 variant corresponding to the amino acids 291–303 of the fusion protein derived from the frameshift DYRK4 peptide (GLKWMLKSQGNVI) was used for immunization. Rabbits were immunized with the fusion-specific peptide conjugated with carrier protein KLH (Keyhole Limpet Hemocyanin) for four times. After immunization, the antibodies were isolated by affinity chromatography using the peptide immobilized on solid support and 1:1000 dilution was used for western blot analysis.

Immunoprecipitation.

The cells were seeded in 10 cm^2 dishes with 200ng/ml for one week. After one week doxycycline treatment, doxycycline-induced T47D OE cells were freshly harvested and lysed in NETN-400 buffer (50 nM Tris-HCL, pH 8.0, 400 nM NaCl, 1 mM EDTA, and 0.5% Nonidet P-40) for 25 minutes on ice and then centrifugated for 25 minutes at 14,500 rpm. The supernatants were diluted with the same buffer without NaCl (NETN-0) to obtain a final concentration of NaCl at 150 mM and incubated with indicated antibodies for 2 hours at 4°C, and then added protein-G beads (Santa Cruz) overnight. The beads were washed three times with cell lysis buffer and the precipitated proteins were subjected to western blot analysis.

Subcellular fractionation.

Upon siRNA treatment completion, cells were harvested and nuclear and cytoplasmic portions were extracted and separated using the NE-PER® Nuclear and Cytoplasmic Extraction reagents (Thermo Scientific) following the manufacturer's instructions. Protein concentration were measured by Micro BCA Protein Assay Kit (Thermo Scientific).

Cell proliferation assay.

T47D cells expressing E9-E2 or wtRAD51AP1 were seeded at a density of 1000cells/well in a 96-well plate with or without 200ng/ml doxycycline treatment. The fusion-negative ZR-75–30 luminal breast cancer and MCF12A benign breast epithelial cell lines were used as negative controls. Cell proliferation was measured by MTS assay at different time points using CellTiter®96Aqueous (Promega) proliferation assay according to manufacturer's instructions. For the data shown in Supplementary Fig. S6A, cell proliferation was measured by MTT Cell Proliferation Kit I (Roche) according to manufacturer's instructions.

Clonogenic assay.

The E9-E2 and wtRAD51AP1 expressing T47D cells were seeded at a density of 1000 cells/well in a 6-well plate with or without 200ng/ml doxycycline treatment and incubated for 14–21 days. The colonies were stained with 0.5% crystal violet in 50% ethanol and counted using GelCount (Oxford Optronix Ltd.). The Trametinib (MEKi) and Lapatinib (EGFR/HER2 inhibitor) used for *in vitro* therapeutic studies were purchased from Selleck Chemicals. To test their therapeutic effects in the engineered T47D cells and other cell lines, cells (5000–10000, depending on the doubling time) were plated in 24-well for 24 hours prior to treatment with growth media containing trametinib, lapatinib or DMSO was replaced every 4 days for approximately 2 weeks. After this, cells were stained with 0.5% crystal violet in water containing 50% ethanol for 15 minutes at room temperature. The area and intensity of each well was measured using Image J. with Colony Area Plug In.

Soft-agar colony formation assay.

The E9-E2 and wtRAD51AP1 expressing T47D cells were suspended in growth medium containing 0.35% SeaPlaque Agarose (Lonza), and plated at a density of 5000 cells/well in a 6-well plate containing 0.7% base agar in growth medium. The cells were then incubated for 21–30 days, and colonies were counted using GelCount.

Migration and transendothelial migration assay.

Transwell migration assay and transendothelial migration assay were performed as described earlier with minor modification (6,14). Both of these assays were performed using Boyden chambers (BD Biosciences). The E9-E2 or wtRAD51AP1 expression was induced in transduced T47D cells with or without 200ng/ml doxycycline for one week. After one-week doxycycline treatment, serum starve the cells overnight. The cells seeded at a density of 2–4×10^5 in serum-free medium onto 8μm pore size transwell inserts placed in 24-well plates containing culture medium with 20% FBS. After 48–72 h, the inserts were removed and stained with hematoxylin. For transendothelial migration assay, HUVECs were seeded in 8μm transwell inserts and incubated overnight. The serum-starved doxycycline-induced T47D OE cells were seeded on top of confluent HUVEC-coated transwell inserts placed in 24-well containing culture medium with 20% FBS. After 48–72h, removed the inserts and the cells were stained as described above. For the data shown in Fig. 2E, the cells were seeded at a density of 4×10^5 in serum-free medium onto 8μm pore size transwell inserts placed in 24-well pates containing culture medium with 20% FBS and 30ng/ml EGF (Sigma-Aldrich). After 48 h incubation, the inserts were removed and stained with 0.1%

crystal violet in 50% methanol for counting using CCD camera associated microscopy (Olympus) and ImageJ.

FACS analysis.

For cell cycle analysis, propidium iodide-stained cells were analyzed in a LSRFortessa cell analyzer (BD Biosciences), and cell cycle phases were calculated using FlowJo (www.flowjo.com).

Statistical analysis.

The results of all *in vitro* experiments were analyzed by student's t-tests or two-way analysis of variance, and all data are shown as mean ± standard deviation.

RESULTS

Discovering chimerical transcripts enriched in luminal B breast cancer

In our previous study, we have developed a fusion-zoom pipeline that identifies pathological recurrent gene fusions from RNAseq and copy number datasets (6). In this study, to detect tumor-specific fusion transcripts, we leveraged the RNAseq analysis module of the fusion-zoom pipeline to identify the chimerical sequences that are abundantly and frequently present in tumor samples but are not expressed in paired normal breast samples. The paired-end RNAseq data for 1059 breast tumors and 111 paired normal breast tumors were obtained from The Cancer Genome Atlas and were aligned with the reference genome using parameters allowing for the detection of fusion transcripts between adjacent genes. A total of 1206 somatic recurrent fusion transcripts were identified, and their preferential presence in luminal B tumors vs luminal A tumors was assessed by two-proportion Z-statistics. A total of 90 candidates were found to be enriched in luminal B tumors, which were then ranked by their frequency of detection in breast tumors, and the median number of supporting reads in tumors (Fig. 1A). The fusion candidates were also evaluated by the concept signature (ConSig) score of the partnering genes to prioritize the biologically meaningful fusions(11,15). The ConSig analysis employs molecular concepts characteristic of cancer genes for computationally assessing the biological function of candidate genes in cancer (11). Among all chimerical transcripts, the most frequent and abundant chimeras enriched in luminal B tumors were *GAL3ST2-NEU4* and *RAD51AP1-DYRK4* (Supplementary Table S1) with *RAD51AP1-DYRK4* showing a higher ConSig score. The fusion partners, RAD51 associated protein 1 (*RAD51AP1*) and Dual-specificity tyrosine-(Y)-phosphorylation regulated kinase 4 (*DYRK4*), are co-linearly placed neighboring genes located approximately 2kb apart on the same strand of chromosome 12, and we did not detect copy number aberrations at RAD51AP1-DYRK4 loci in the fusion positive tumors (Supplementary Fig. S1). These suggest that this fusion may be a neoplastic read-through event.

RAD51AP1 is a RAD51-interacting protein specific to the vertebrates. Several studies have shown the involvement of RAD51AP1 in homologous recombination (HR) repair through its interaction with RAD51(16,17). Besides its role in HR repair, enhanced expression of RAD51AP1 has been found to be involved in the growth of intrahepatic cholangiocarcinoma

(18). DYRK4 belongs to a conserved family of serine/threonine protein kinases (19); this gene, however, does not contribute any in-frame protein sequences to the fusion protein product. Therefore, it is highly unlikely that the fusion protein act through DYRK4 kinase activity or serve as dominant negative of DYRK4. Among the 1059 breast tumors sequenced by TCGA, *RAD51AP1-DYRK4* chimeric transcript is detected in 38 tumors (3.59 %), and is preferentially present in luminal B tumors (7%, 13/192) compared to luminal A tumors (3%, 11/418) (Supplementary Table S1–2).

Tumor-specific *RAD51AP1-DYRK4* transcripts are ectopically overexpressed in luminal breast cancers.

To assess the expression of *RAD51AP1-DYRK4* in breast tumor samples, we examined 200 ER+ breast tumor tissues and a panel of breast cancer cell lines by reverse transcription PCR (RT-PCR) using forward primers from Exon 1 of *RAD51AP1* and reverse primers from exon 2 of *DYRK4* that can detect all of the aforementioned variants (Fig. 1B, Supplementary Fig. S2). Of the 200 ER+ tumors analyzed, strong *RAD51AP1-DYRK4* expression was detected in 19 tumors (9.5%), which was verified by capillary sequencing (Supplementary Table S3). *RAD51AP1-DYRK4* expression tends to be mutually exclusive with ESR1-CCDC170, suggesting that this fusion could be independent pathological events in luminal B breast cancer (Fig. 1C). The fusion transcripts are not detected in the paired adjacent normal breast tissues, suggesting their high tumor-specificity (Fig. 1D). To investigate the expression of *RAD51AP1-DYRK4* in normal tissues, RT-PCR was performed in 23 types of pooled normal human tissues, including somatic, germ, and fetal tissues. The *RAD51AP1-DYRK4* transcript was expressed abundantly in testis, and marginally in thymus, but not in any of the other 21 tissues examined (including breast, ovary, and uterus, Fig. 1E). Such cancer-testis specific expression pattern implies an important function role of *RAD51AP1-DYRK4* in breast cancer as we and others previous reported(20–22). It is notable that *RAD51AP1-DYRK4* expression tend to present in the tumors overexpressing wt*RAD51AP1*, but not vice versa. This suggests that an active RAD51AP1 promoter may act as a prerequisite for the expression of this fusion, but not all samples with active RAD51AP1 promoter express this chimerical transcript.

RAD51AP1-DYRK4 is preferentially overexpressed in luminal B breast tumors.

High Ki67 proliferation index is a biomarker for luminal B tumors, and cutoff of 13~15% positivity is clinically used to differentiate luminal B tumors (23–25). In our previous study (6), we have performed Ki67 immunohistochemistry on 193 out of the 200 ER+ tumor tissues that we have tested for *RAD51AP1-DYRK4*. We thus assessed the association of *RAD51AP1-DYRK4* expression with the Ki67 index. In line with the observation from TCGA tumors, the *RAD51AP1-DYRK4*-positive tumors displayed a significantly higher Ki67 index than the negative cases (p=0.004) (Fig. 1F, upper panel), suggesting a significant association of *RAD51AP1-DYRK4* with the luminal B subtype. While weak expression of *RAD51AP1-DYRK4* was observed in an additional 93 ER^+ breast tumors (we termed as intermediate cases), these cases did not demonstrate a significantly increased Ki67 index (p=0.297). Thus, only strong overexpressing cases are considered as fusion-positive in the following studies, which are determined based on RT-PCR band intensities (Supplementary Fig. S3). Using 15% Ki67 positivity as cutoff, 80 tumors have high Ki67 index, among

which 14 cases are fusion-positive (17.5%). Among the 113 Ki67-low tumors, only 5 tumors are fusion-positive (4.4%). Fisher's exact test suggests a significant enrichment of positive cases in Ki67 high tumors (p=0.006). Next, we compared the Ki67 index between *RAD51AP1-DYRK4+* tumors and the wt*RAD51AP1* overexpressing tumors. This revealed a significantly higher Ki67 index in *RAD51AP1-DYRK4* + tumors compared to wt*RAD51AP1* overexpressing tumors (p=0.046) (Fig. 1F, lower panel).

Since RT-PCR analysis revealed *RAD51AP1-DYRK4* expression in many triple-negative breast cancer (TNBC) cell lines (Supplementary Fig. S2), we examined the expression of RAD51AP1-DYRK4 in 45 primary triple-negative breast tumors which however, revealed only two RAD51AP1-DYRK4 positive cases (Supplementary Fig. S4). This suggests low RAD51AP1-DYRK4 positivity in primary TNBC tumors.

Characterization of *RAD51AP1-DYRK4* encoded protein products

Next, we sought to characterize the protein products encode by RAD51AP1-DYRK4. RNAseq and RT-PCR detected three major intergenic splicing variants in the breast tumors and cell lines, namely E9-E2, E8-E2, or E8s-E2 variant transcripts, in which exon 9, 8, or an alternative splicing donor site in exon 8 of *RAD51AP1* is fused to exon 2 of *DYRK4*, with the E9-E2 variant being most frequently detected in breast tumors. As a common scheme, the *RAD51AP1-DYRK4* variants encode a C-terminally truncated RAD51AP1 protein fused to a short fragment of frame-shift peptide translated from the DYRK4 portion (Fig. 2A), leading to the loss of RAD51 interacting domain. To test the translatability of *RAD51AP1-DYRK4* transcripts in breast cancer, we engineered the fusion cDNA containing the most common variant E9-E2 chimeric ORF together with the endogenous 5' translation start sequences into a doxycycline-inducible lentiviral vector, which was then transduced into the T47D luminal- A like breast cancer cells. Western blot analysis using a commercial polyclonal antibody against the N-terminus of RAD51AP1 detected the E9-E2 or wtRAD51AP1 protein bands specific to the transduced T47D cells treated with doxycycline (Fig. 2B). Of note, both E9-E2 and wtRAD51AP1 overexpressing T47D cells exhibited two specific protein bands respectively. To verify the identity of these E9-E2 and wtRAD51AP1 protein bands, we transfected the engineered T47D cells with 5'RAD51AP1 siRNA designed to knockdown both RAD51AP1-DYRK4 and wtRAD51AP1, or the 3'RAD51AP1 siRNA designed to only inhibit the wtRAD51AP1. Subsequent western blots showed that the 5'siRNA but not 3'siRNA silenced both the E9-E2 bands and the wtRAD51AP1 bands induced by doxycycline, which verified the identities of these bands (Fig. 2B). To examine if the DYRK4 coding sequence following the fusion ORF can be translated from the *RAD51AP1-DYRK4* transcript, we added a Flag-tag to the 3' end of the fusion ORF or the 3' end of the DYRK4 ORF. Immunoblots of T47D cells transfected with these constructs using an anti-Flag antibody detected the fusion protein but not DYRK4 protein (Supplementary Fig. S5). This suggests that the fusion transcripts do not encode DYRK4 protein.

RAD51AP1-DYRK4 promotes cancer cell motility and trans-endothelial migration.

We then explored the phenotypic changes in the T47D luminal breast cancer cells inducibly overexpressing RAD51AP1-DYRK4 or wtRAD51AP1. Since all chimeric variants encode

similar c-terminal truncated RAD51AP1 protein fused to a frame-shift peptide from DYRK4 (Fig. 2A), and are often detected in the same tumors presumably due to alternative intergenic-splicing events (Fig. 1B), we focused our following functional studies on one most common variant, E9-E2. Transwell migration assays suggested that RAD51AP1-DYRK4 but not wtRAD51AP1 significantly augments the chemotactic migration of T47D breast cancer cells (Fig. 2C). On the other hand, RAD51AP1-DYRK4 did not confer increased cell proliferation or colony-forming capability, whereas wtRAD51AP1 decreased the cell proliferation and colony formation, and increased the G1 cell population (Supplementary Fig. S6). To mimic the *in vivo* behavior of tumor cells undergoing extravasation during metastasis (26), we performed *in vitro* transendothelial migration assays to test the effect of RAD51AP1-DYRK4 on trans-endothelial migration of breast cancer cells. The T47D cells inducibly expressing RAD51AP1-DYRK4 or wtRAD51AP1 were allowed to migrate through a confluent monolayer of human umbilical vein endothelial cells (HUVECs). Ectopic expression of RAD51AP1-DYRK4 but not wtRAD51AP1 significantly enhanced the trans-endothelial migration of T47D cells (Fig. 2D). To assess if RAD51AP1-DYRK4 function is dependent on wtRAD51AP1, we performed specific knockdown of wtRAD51AP1 using two siRNAs against its 3' region not involved in the fusion in the T47D cells inducibly overexpressing RAD51AP1-DYRK4 (Fig. 2E). Our result showed that the cell motility is not significantly affected by depletion of wtRAD51AP1 in the presence or absence of exogenous overexpression of the fusion. These data suggest that RAD51AP1-DYRK4 but not wtRAD51AP1 promotes motility and transendothelial migration of luminal breast cancer cells, and the function of the fusion does not depend on the wild-type protein.

Augmented MEK/ERK signaling is characteristic of RAD51AP1-DYRK4 expressing breast tumors.

To examine the signaling alterations differentially associated with RAD51AP1-DYRK4 or wtRAD51AP1 expression, immunoblots were performed on the T47D cells ectopically expressing RAD51AP1-DYRK4 or wtRAD51AP1 (Fig. 3A). As a result, we observed substantially increased phosphorylation of MEK/ERK following RAD51AP1-DYRK4 overexpression in T47D cells. Upregulation of integrin B1 (ITGB1) was also observed in fusion-expressing T47D cells. Most of these changes are specific to the RAD51AP1-DYRK4 overexpressing T47D cells, compared to wtRAD51AP1. To explore the impact of extracellular matrix on MEK/ERK signaling associated with RAD51AP1-DYRK4 expression, we examined the signaling alterations in the engineered T47D cells cultured in Matrigel, a solubilized basement membrane preparation rich in ECM proteins (i.e. laminin, collagen IV)(27). Interestingly, with extracellular matrix, the activation of the MEK/ERK cascade were markedly enhanced (Fig. 3A). In addition, this enhancement is highly specific to the T47D cells expressing RAD51AP1-DYRK4 --- it is not observed in wtRAD51AP1-expressing T47D cells. This suggests that in the breast tumor tissues containing extracellular matrix, RAD51AP1-DYRK4 may play a key role in activating the MEK-ERK signaling. Further, TCGA breast cancer reverse phase protein array (RPPA) data revealed that the fusion-expressing tumors displayed a significantly increased phosphorylation of MEK/ERK, compared to wtRAD51AP1 overexpressing luminal B tumors which support our observations on the T47D ectopic expression model (Fig. 3B).

To identify the key molecules important for RAD51AP1-DYRK4 to modulate MEK signaling, we investigated the RAD51AP1 interactants with the Entrez Gene database. This revealed a potential RAD51AP1 interactant, MAP3K1, a cytoplasmic protein that regulates ERK, JNK, and p38, and is known to suppress metastasis and induce anoiksis (28). We thus performed immuno-precipitation using the RAD51AP1 antibody in the T47D cells overexpressing E9-E2 or wtRAD51AP1. Our result showed that MAP3K1 protein co-precipitated with both wtRAD51AP1 and E9-E2 proteins, suggesting their direct functional relations (Fig. 3C). On the other hand, other known MEK upstream signaling proteins such as ErBb receptor kinases, integrin β1, c-Src, or MEK itself did not co-precipitate with RAD51AP1-DYRK4.

Assessing the function of endogenous RAD51AP1-DYRK4 protein in luminal breast cancer cells.

Next, we sought to assess the function of endogenous RAD51AP1-DYRK4 protein overexpressed in MDAMB361 (Supplementary Fig. S7A). MDAMB361 is an ER+/Her2+ cell line derived from brain metastasis (29) and is resistant to endocrine or her2-targeted therapies (30,31). We thus used this cell line as a model to study the function of the endogenous RAD51AP1-DYRK4. To specifically knockdown RAD51AP1-DYRK4, we designed several siRNAs targeting the fusion junctions, which however, appear to have general toxicity to the cells. We therefore designed two 5'RAD51AP1 siRNAs that knockdown both RAD51AP1-DYRK4 and wtRAD51AP1, and two DYRK4 siRNAs targeting both RAD51AP1-DYRK4 and wtDYRK4, and two 3'RAD51AP1 siRNAs designed to only inhibit the wtRAD51AP1 (Fig. 4A). We then performed Western blot analysis to detect the endogenously expressed RAD51AP1-DYRK4 protein products in the MDA-MB-361 cells. As a result, we were able to readily detect the E9-E2 protein band expressed by the MDAMB361 cells, which can be inhibited by the 5'RAD51AP1 siRNAs and DYRK4 siRNAs, but not by 3'RAD51AP1 siRNAs (Fig. 4B). The levels of the protein inhibitions appear to correlate with the levels of transcript inhibitions by these siRNAs detected by qPCR (Supplementary Fig. S7B).

To further verify the identity of the endogenous E9-E2 protein band, we generated a polyclonal antibody against the frameshift DYRK4 peptide, which can specifically detect RAD51AP1-DYRK4 but not wtRAD51AP1. Western blots using this antibody on the MDAMB361 cells detected the previously identified fusion-protein band, which can be inhibited by the siRNAs that can repress the fusion (Supplementary Fig. S8). This verified the identity of the fusion protein band and further support that the frame-shift peptide derived from DYRK4 instead of the wild-type DYRK4 protein sequence are translated from the DYRK4 portion of the chimerical transcript. We then examined the localization of the endogenous RAD51AP1-DYRK4 in the nuclear or cytoplasmic fractions of MDAMB361 cells. The E9-E2 protein preferentially localizes to cytoplasm, in contrast to the nuclear localization of wtRAD51AP1 (Fig. 4C). This result is consistent with the distinct function of the fusion in modulating cytoplasmic signaling in contrast to the role of wtRAD51AP1 in HR repair.

To further assess the function of the endogenous RAD51AP1-DYRK4 protein, we selected the fusion-positive MDAMB361 cells and the fusion-negative cell line ZR75–30 and MCF12A (Supplementary Fig. S7A), transfected these cell lines with the selected siRNAs targeting 5'RAD51AP1, 3' RAD51AP1, or DYRK4, and performed MTS assay (Fig. 4D). The cell proliferation is significantly inhibited by the 5'RAD51AP1 siRNA, and by two DYRK4 siRNAs, but not by the 3'RAD51AP1 siRNA specific to wtRAD51AP1. Such effects are not observed in the negative control cell lines ZR75–30, and MCF12A cells, which verified the specific functional effects of the siRNAs against RAD51AP1-DYRK4. Next, we performed western blots following siRNA treatments to examine the function of the endogenously expressed RAD51AP1-DYRK4 on modulating MEK/ERK signaling in the MDAMB361 model (Fig. 4E). Our result showed that the siRNAs against 5'RAD51AP1 or DYRK4 (targeting RAD51AP1-DYRK4), but not 3'RAD51AP1 (targeting wtRAD51AP1) lead to repression of MEK/ERK signaling. This further support the function of the endogenously expressed RAD51AP1-DYRK4 on regulating MEK/ERK signaling.

RAD51AP1-DYRK4 endows increased sensitivity to MEK inhibition and attenuates MEKi induced HER2/PI3K/AKT activation

Next, we sought to assess the sensitivity of the engineered T47D cells inducibly expressing RAD51AP1-DYRK4 or wtRAD51AP1 to MEK inhibition. Here we chose the first FDA approved MEK inhibitor currently under phase II clinical trial for triple negative breast cancer (NCI 9455) called Trametinib. As suggested by the previous study, MEK inhibition requires longer term drug exposure to exert therapeutic effect(32). We thus performed clonogenic assays on the T47D models to assess the cell viability following trametinib treatment in the presence or absence of doxycycline induction. Since T47D cells express EGFR, we also treated the cells with lapatinib to observe the combinatory effect. As a result, ectopic expression of RAD51AP1-DYRK4 resulted in significantly increased sensitivity to trametinib, which is not observed following induction of wtRAD51AP1 expression (Fig. 5A). Lapatinib alone or in combination with trametinib did not result in additional therapeutic benefits.

Next, we assessed the trametinib sensitivity in a panel breast cancer cells lines with variable levels of endogenous RAD51AP1-DYRK4 as assessed by real-time PCR (Supplementary Fig. S7A). As Shown by clonogenic assays, the MDAMB361 and HCC1937 cell lines overexpressing RAD51AP1-DYRK4 showed markedly higher sensitivity to trametinib treatment compared to MCF7, HCC38, HCC1428, and ZR-75–30 cell lines (Fig. 5B). Since MDAMB361 is a HER2 positive cell line we also assessed the therapeutic effect of lapatinib treatment alone or in combination with trametinib. MDAMB361 appeared highly resistant to lapatinib, and the combination treatment yielded similar therapeutic effect as trametinib alone (Fig. 5C). These data suggest that RAD51AP1-DYRK4 endows increased sensitivity to MEK inhibition in the luminal breast cancer cells overexpressing ectopic or endogenous RAD51AP1-DYRK4.

Since inactivating mutations of MAP3K1, which account for about 9% of breast cancer (5,33), has been found to confer increased sensitivity to MEK inhibition(32), here we assessed the mutual exclusivity of RAD51AP1-DYRK4 with MAP3K1 mutation based on

the somatic mutation data for TCGA tumors (Supplementary Fig. S9). Of the 1059 TCGA tumors analyzed, 81 are MAP3K1 mutation positive and 37 are RAD51AP1-DYRK4 positive, whereas only 2 cases are found to be positive for both, suggesting these as independent events (Fisher's exact test of dependence: p=1).

Compensative HER2/PI3K/AKT and MAP3K1/JNK/JUN activation has been reported to mediate resistance to MEK inhibitors(32,34). We thus examined if RAD51AP1-DYRK4 and wtRAD51AP1 differentially modulate these survival pathways following MEK inhibition. To test this, we treated the engineered T47D cells with 0.5uM of trametinib or vehicle for 24 hours, to assess the early signaling changes following trametinib treatment. Western blot analysis revealed that, under MEK inhibition, RAD51AP1-DYRK4 attenuated HER2/PI3K/AKT/Raptor activation in the T47D cells overexpressing RAD51AP1-DYRK4. In contrast, this compensatory signaling was activated in T47D cells overexpressing wtRAD51AP1 following MEK inhibition (Fig. 6A). In addition, RAD51AP1-DYRK4 also repressed MAP3K1 protein level and JNK-JUN phosphorylation under MEK inhibition. However, we did not observe activation of this signaling following MEK inhibition in the T47D cells ectopically expressing wtRAD51AP1. These results suggest that RAD51AP1-DYRK4 may endow sensitivity to MEK inhibition via repressing compensatory HER2/PI3K/AKT activation (Fig. 6B).

DISCUSSION

To date, the pathological molecular events underlying the aggressive and metastatic form of luminal breast cancer remain poorly understood. In addition, the recent genome sequencing studies have revealed a paucity of actionable drivers in these tumors (5). Here we report a non-traditional cancer-testis specific fusion transcript RAD51AP1-DYRK4 which is frequently and preferentially expressed in luminal B tumors. Consistent with our results, a most recent landscape study of chimeric transcripts in 9495 non-diseased samples of 53 different human tissue types sequenced by the Genotype-Tissue Expression project cataloged RAD51AP1-DYRK4 as a testis specific chimera, which is also detected in EBV-transformed cells(35). This implies a potential connection between testis, luminal B breast cancer, and virus transformation. In addition, in our previous study, we analyzed WGS data from International Cancer Genome Consortium (ICGC) for 215 breast tumors to detect recurrent gene rearrangements(36). Among these 92 breast tumors are contributed by The Cancer Genome Atlas (TCGA)(36), and six of these are detected as RAD51AP1-DYRK4 positive by matched RNAseq data. However, we did not detect any genomic rearrangements between RAD51AP1 and DYRK4 loci in all these 215 breast tumors. Combined with the fact that no copy number changes are detected in the intergenic regions between RAD51AP1 and DYRK4 in the TCGA positive cases (Supplementary Fig. S1), and that *RAD51AP1* are co-linearly placed neighboring genes located ~2kb apart on the same strand, this chimera is highly likely to be a neoplastic read-through event.

While read-through chimeras including *SLC45A3–ELK4* have been found to be overexpressed in specific tumor entity (37–39), highly tumor-specific read-through events like *RAD51AP1-DYRK4* that are silent in human somatic tissues but are overexpressed in testis and specific tumor entities have not been previously identified in breast cancer.

Cancer-testis specific genes have been found to play an important role in breast cancer pathobiology and therapeutic response as represented by the HORMAD1 protein we and others reported previously (20–22). Our discovery of RAD51AP1-DYRK4 sheds light on a new area of the molecular pathobiology of luminal B breast cancer, by revealing a novel cancer-testis specific chimerical transcript underlying their aggressive behaviors and sensitivity to MEK inhibition. While it will be interesting to further verify the splicing mechanism generating this chimera, this aspect will be out of the scope of the present study focusing on the pathological and therapeutic role of RAD51AP1-DYRK4 in more aggressive luminal breast cancer. Future studies will be required to pinpoint the transcriptional mechanisms generating this chimera.

RAD51AP1-DYRK4 encodes c-terminal truncated RAD51AP1 protein fused to a small frame-shift peptide from DYRK4, resulting in a cytoplasmic localized protein that lacks the RAD51 interacting domain. The truncation of RAD51AP1 and the addition of a frameshift DYRK4 peptide resulting from this fusion may twist the biology of RAD51AP1. Herein, we provide molecular evidence that RAD51AP1-DYRK4 expression is highly tumor-specific and is markedly enriched in ER+ luminal B breast tumors (7–18%) compared to luminal A tumors (3–4%). Of note, the lower detection rate of RAD51AP1-DYRK4 in TCGA tumors could be attributed to the short read-length (50 bp) and low sequencing depth of TCGA RNAseq data that limits the sensitivity of fusion detection. Ectopic expression of RAD51AP1-DYRK4, but not wild-type (wt) RAD51AP1, endows increased motility and transendothelial migration of luminal breast cancer cells, and the function of RAD51AP1-DYRK4 does not appear to depend on the wild-type protein. Moreover, we have identified the endogenous RAD51AP1-DYRK4 protein expressed in fusion-positive cells, silencing of which leads to decreased cell viability.

Furthermore, our finding of RAD51AP1-DYRK4-mediated activation of MEK/ERK signaling known to regulate breast cancer migration (40) and anoiksis resistance (41), emphasizes the potential significance and functional implications of RAD51AP1-DYRK4 in breast cancer invasiveness and metastasis. More interestingly, our data show that RAD51AP1-DYRK4 forms complex with MAP3K1 and endow sensitivity to the MEK inhibitor (MEKi) Trametinib via attenuating compensatory HER2/PI3K/AKT activation (Fig. 6B). The expression of RAD51AP1-DYRK4, but not wtRAD51AP1 appears to negatively correlate with MAP3K1 protein level as shown by the western blots detecting MAP3K1 following silencing or overexpressing the fusion (Fig. 4E, 6A). Future studies will be required to pinpoint the precise mechanism engaged by RAD51AP1-DYRK4 to endow cancer cell addiction to MEK/ERK signaling, and the interplay between RAD51AP1-DYRK4/MAP3K1 and HER2/PI3K/AKT signaling.

It is noteworthy that RAD51AP1 has been previously reported to be a critical molecule for homologous recombination (HR) DNA repair by interacting with and stimulating RAD51 and DMC1 recombinase activity in mitotic and meiotic cells (16,17). Our present study points out the importance of RAD51AP1-DYRK4 in cytoplasmic signaling, presumably due to the loss of RAD51 interacting domain and preferential localization to the cytoplasm. Nonetheless, it will be interesting to further explore whether RAD51AP1-DYRK4 impairs RAD51AP1-mediated HR repair and enhances the genomic instability of luminal B breast

cancers. In addition, future studies will be required to further evaluate the pathological role of wtRAD51AP1 in luminal B breast cancer.

Effective predictive and therapeutic approaches to circumvent the potential impediments in the treatment of luminal B tumors, is yet to be developed. We expect that targeting of the fusion driven MEK signaling may offer potential new therapeutic opportunities for a substantial population of patients with deadly luminal breast tumors. Future studies will be required to further establish the synthetic lethality between RAD51AP1-DYRK4 overexpression and MEK sensitivity in preclinical and clinical studies.

CONCLUSIONS

In this study, our large-scale analysis of TCGA RNAseq data revealed novel neoplastic RAD51AP1-DYRK4 fusion transcript ectopically and preferentially expressed in luminal B breast cancer. This discovery sheds light on a new area of molecular pathobiology of luminal B tumors, by revealing a new form of molecular events that may confer their aggressiveness and metastasis-prone behaviors. To our knowledge, RAD51AP1-DYRK4 fusion could be the most frequently expressed tumor-specific fusion transcript reported in luminal breast tumors. This study also suggests the potential of targeting the fusion-driven MEK signaling in the management of RAD51AP1-DYRK4 expressing luminal breast tumors.

Supplementary Material

Refer to Web version on PubMed Central for supplementary material.

Acknowledgements

This study was supported by NIH grant 1R01CA181368 (X-S. Wang.), 1R01CA183976 (X-S. Wang.), 1R21CA237964 (X-S. Wang.), Congressionally Directed Medical Research Programs W81XWH-13-1-0431 (J. Veeraraghavan), Susan G. Komen foundation PDF12231561 (J. Kim.), PDF15333523 (X. Wang), Commonwealth of PA Tobacco Phase 15 Formula Fund (X-S. Wang), the Shear Family Foundation (X-S. Wang), the Hillman Foundation (X-S. Wang), and development funds from Cancer Center support grant P30 CA047904 and SPORE P50 CA159981 (X-S. Wang). We thank Dr. Rachel Schiff for helpful discussions and Dr. Ling Lin for the help with western blots. The results published here are in part based upon data generated by The Cancer Genome Atlas project established by the NCI and NHGRI (dbGaP accession: phs000178.v6.p6). The computational infrastructure was supported by the Dan L. Duncan Cancer Center Computational Facility and the Rice University BlueBioU Computer Cluster (supported by a 2010 IBM Shared University Research Award on IBM's Power7 high performance cluster, and the NIH grant NCRR S10RR02950). The NCI/ATTC 45 breast cancer cell line kit was provided by the Antibody-Based Proteomic Shared Resource of the Dan L. Duncan Comprehensive Cancer Center (supported by P30CCSG CA125123).

REFERENCES

1. Yersal O, Barutca S. Biological subtypes of breast cancer: Prognostic and therapeutic implications. World J Clin Oncol 2014;5(3):412–24 doi 10.5306/wjco.v5.i3.412. [PubMed: 25114856]
2. Goksu SS, Tastekin D, Arslan D, Gunduz S, Tatli AM, Unal D, et al. Clinicopathologic features and molecular subtypes of breast cancer in young women (age </=35). Asian Pac J Cancer Prev 2014;15(16):6665–8 doi 10.7314/apjcp.2014.15.16.6665. [PubMed: 25169505]
3. Ades F, Zardavas D, Bozovic-Spasojevic I, Pugliano L, Fumagalli D, de Azambuja E, et al. Luminal B breast cancer: molecular characterization, clinical management, and future perspectives. J Clin Oncol 2014;32(25):2794–803 doi 10.1200/JCO.2013.54.1870. [PubMed: 25049332]
4. Sotiriou C, Pusztai L. Gene-expression signatures in breast cancer. The New England journal of medicine 2009;360(8):790–800 doi 10.1056/NEJMra0801289. [PubMed: 19228622]

5. Koboldt DC, Fulton RS, McLellan MD, Schmidt H, Kalicki-Veizer J, McMichael JF, et al. Comprehensive molecular portraits of human breast tumours. Nature 2012 doi 10.1038/nature11412.
6. Veeraraghavan J, Tan Y, Cao XX, Kim JA, Wang X, Chamness GC, et al. Recurrent ESR1-CCDC170 rearrangements in an aggressive subset of oestrogen receptor-positive breast cancers. Nat Commun 2014;5:4577 doi 10.1038/ncomms5577. [PubMed: 25099679]
7. Fimereli D, Fumagalli D, Brown D, Gacquer D, Rothe F, Salgado R, et al. Genomic hotspots but few recurrent fusion genes in breast cancer. Genes Chromosomes Cancer 2018;57(7):331–8 doi 10.1002/gcc.22533. [PubMed: 29436103]
8. Giltnane JM, Hutchinson KE, Stricker TP, Formisano L, Young CD, Estrada MV, et al. Genomic profiling of ER(+) breast cancers after short-term estrogen suppression reveals alterations associated with endocrine resistance. Sci Transl Med 2017;9(402) doi 10.1126/scitranslmed.aai7993.
9. Matissek KJ, Onozato ML, Sun S, Zheng Z, Schultz A, Lee J, et al. Expressed Gene Fusions as Frequent Drivers of Poor Outcomes in Hormone Receptor-Positive Breast Cancer. Cancer Discov 2018;8(3):336–53 doi 10.1158/2159-8290.CD-17-0535. [PubMed: 29242214]
10. Hartmaier RJ, Trabucco SE, Priedigkeit N, Chung JH, Parachoniak CA, Vanden Borre P, et al. Recurrent hyperactive ESR1 fusion proteins in endocrine therapy-resistant breast cancer. Ann Oncol 2018;29(4):872–80 doi 10.1093/annonc/mdy025. [PubMed: 29360925]
11. Wang XS, Prensner JR, Chen G, Cao Q, Han B, Dhanasekaran SM, et al. An integrative approach to reveal driver gene fusions from paired-end sequencing data in cancer. Nat Biotechnol 2009;27(11):1005–11 doi 10.1038/nbt.1584. [PubMed: 19881495]
12. Li J, Lu Y, Akbani R, Ju Z, Roebuck PL, Liu W, et al. TCPA: a resource for cancer functional proteomics data. Nature methods 2013;10(11):1046–7 doi 10.1038/nmeth.2650.
13. Uphoff CC, Drexler HG. Detecting mycoplasma contamination in cell cultures by polymerase chain reaction. Methods Mol Biol 2011;731:93–103 doi 10.1007/978-1-61779-080-5_8. [PubMed: 21516400]
14. Cen J, Feng L, Ke H, Bao L, Li LZ, Tanaka Y, et al. Exosomal Thrombospondin-1 Disrupts the Integrity of Endothelial Intercellular Junctions to Facilitate Breast Cancer Cell Metastasis. Cancers (Basel) 2019;11(12) doi 10.3390/cancers11121946.
15. Kim JA, Tan Y, Wang X, Cao X, Veeraraghavan J, Liang Y, et al. Comprehensive functional analysis of the tousled-like kinase 2 frequently amplified in aggressive luminal breast cancers. Nat Commun 2016;7:12991 doi 10.1038/ncomms12991. [PubMed: 27694828]
16. Wiese C, Dray E, Groesser T, San Filippo J, Shi I, Collins DW, et al. Promotion of homologous recombination and genomic stability by RAD51AP1 via RAD51 recombinase enhancement. Molecular cell 2007;28(3):482–90 doi 10.1016/j.molcel.2007.08.027. [PubMed: 17996711]
17. Dunlop MH, Dray E, Zhao W, Tsai MS, Wiese C, Schild D, et al. RAD51-associated protein 1 (RAD51AP1) interacts with the meiotic recombinase DMC1 through a conserved motif. The Journal of biological chemistry 2011;286(43):37328–34 doi 10.1074/jbc.M111.290015. [PubMed: 21903585]
18. Obama K, Satoh S, Hamamoto R, Sakai Y, Nakamura Y, Furukawa Y. Enhanced expression of RAD51 associating protein-1 is involved in the growth of intrahepatic cholangiocarcinoma cells. Clin Cancer Res 2008;14(5):1333–9 doi 10.1158/1078-0432.CCR-07-1381. [PubMed: 18316552]
19. Park J, Song WJ, Chung KC. Function and regulation of Dyrk1A: towards understanding Down syndrome. Cellular and molecular life sciences : CMLS 2009;66(20):3235–40 doi 10.1007/s00018-009-0123-2. [PubMed: 19685005]
20. Wang X, Tan Y, Cao X, Kim JA, Chen T, Hu Y, et al. Epigenetic activation of HORMAD1 in basal-like breast cancer: role in Rucaparib sensitivity. Oncotarget 2018;9(53):30115–27 doi 10.18632/oncotarget.25728. [PubMed: 30046392]
21. Watkins J, Weekes D, Shah V, Gazinska P, Joshi S, Sidhu B, et al. Genomic Complexity Profiling Reveals That HORMAD1 Overexpression Contributes to Homologous Recombination Deficiency in Triple-Negative Breast Cancers. Cancer Discov 2015;5(5):488–505 doi 10.1158/2159-8290.CD-14-1092. [PubMed: 25770156]
22. Mahmoud AM. Cancer testis antigens as immunogenic and oncogenic targets in breast cancer. Immunotherapy 2018;10(9):769–78 doi 10.2217/imt-2017-0179. [PubMed: 29926750]

23. Cheang MC, Chia SK, Voduc D, Gao D, Leung S, Snider J, et al. Ki67 index, HER2 status, and prognosis of patients with luminal B breast cancer. Journal of the National Cancer Institute 2009;101(10):736–50 doi 10.1093/jnci/djp082. [PubMed: 19436038]
24. Voduc KD, Cheang MC, Tyldesley S, Gelmon K, Nielsen TO, Kennecke H. Breast cancer subtypes and the risk of local and regional relapse. Journal of clinical oncology : official journal of the American Society of Clinical Oncology 2010;28(10):1684–91 doi 10.1200/JCO.2009.24.9284. [PubMed: 20194857]
25. Tran B, Bedard PL. Luminal-B breast cancer and novel therapeutic targets. Breast cancer research : BCR 2011;13(6):221 doi 10.1186/bcr2904. [PubMed: 22217398]
26. Voura EB, Ramjeesingh RA, Montgomery AM, Siu CH. Involvement of integrin alpha(v)beta(3) and cell adhesion molecule L1 in transendothelial migration of melanoma cells. Molecular biology of the cell 2001;12(9):2699–710. [PubMed: 11553709]
27. Streuli CH, Schmidhauser C, Bailey N, Yurchenco P, Skubitz AP, Roskelley C, et al. Laminin mediates tissue-specific gene expression in mammary epithelia. The Journal of cell biology 1995;129(3):591–603. [PubMed: 7730398]
28. Pham TT, Angus SP, Johnson GL. MAP3K1: Genomic Alterations in Cancer and Function in Promoting Cell Survival or Apoptosis. Genes Cancer 2013;4(11–12):419–26 doi 10.1177/1947601913513950. [PubMed: 24386504]
29. Engel LW, Young NA. Human breast carcinoma cells in continuous culture: a review. Cancer Res 1978;38(11 Pt 2):4327–39. [PubMed: 212193]
30. Antoon JW, White MD, Driver JL, Burow ME, Beckman BS. Sphingosine kinase isoforms as a therapeutic target in endocrine therapy resistant luminal and basal-A breast cancer. Exp Biol Med (Maywood) 2012;237(7):832–44 doi 10.1258/ebm.2012.012028. [PubMed: 22859737]
31. Goel S, Wang Q, Watt AC, Tolaney SM, Dillon DA, Li W, et al. Overcoming Therapeutic Resistance in HER2-Positive Breast Cancers with CDK4/6 Inhibitors. Cancer cell 2016;29(3):255–69 doi 10.1016/j.ccell.2016.02.006. [PubMed: 26977878]
32. Xue Z, Vis DJ, Bruna A, Sustic T, van Wageningen S, Batra AS, et al. MAP3K1 and MAP2K4 mutations are associated with sensitivity to MEK inhibitors in multiple cancer models. Cell Res 2018;28(7):719–29 doi 10.1038/s41422-018-0044-4. [PubMed: 29795445]
33. Avivar-Valderas A, McEwen R, Taheri-Ghahfarokhi A, Carnevalli LS, Hardaker EL, Maresca M, et al. Functional significance of co-occurring mutations in PIK3CA and MAP3K1 in breast cancer. Oncotarget 2018;9(30):21444–58 doi 10.18632/oncotarget.25118. [PubMed: 29765551]
34. Wee S, Jagani Z, Xiang KX, Loo A, Dorsch M, Yao YM, et al. PI3K pathway activation mediates resistance to MEK inhibitors in KRAS mutant cancers. Cancer Res 2009;69(10):4286–93 doi 10.1158/0008-5472.CAN-08-4765. [PubMed: 19401449]
35. Singh S, Qin F, Kumar S, Elfman J, Lin E, Pham LP, et al. The landscape of chimeric RNAs in non-diseased tissues and cells. Nucleic Acids Res 2020;48(4):1764–78 doi 10.1093/nar/gkz1223. [PubMed: 31965184]
36. Lee S, Hu Y, Loo SK, Tan Y, Bhargava R, Lewis MT, et al. Landscape analysis of adjacent gene rearrangements reveals BCL2L14-ETV6 gene fusions in more aggressive triple-negative breast cancer. Proc Natl Acad Sci U S A 2020;117(18):9912–21 doi 10.1073/pnas.1921333117. [PubMed: 32321829]
37. Zhang Y, Gong M, Yuan H, Park HG, Frierson HF, Li H. Chimeric transcript generated by cis-splicing of adjacent genes regulates prostate cancer cell proliferation. Cancer discovery 2012;2(7):598–607 doi 10.1158/2159-8290.CD-12-0042. [PubMed: 22719019]
38. Maher CA, Kumar-Sinha C, Cao X, Kalyana-Sundaram S, Han B, Jing X, et al. Transcriptome sequencing to detect gene fusions in cancer. Nature 2009;458(7234):97–101. [PubMed: 19136943]
39. Nacu S, Yuan W, Kan Z, Bhatt D, Rivers CS, Stinson J, et al. Deep RNA sequencing analysis of readthrough gene fusions in human prostate adenocarcinoma and reference samples. BMC medical genomics 2011;4:11 doi 10.1186/1755-8794-4-11. [PubMed: 21261984]
40. Chen H, Zhu G, Li Y, Padia RN, Dong Z, Pan ZK, et al. Extracellular signal-regulated kinase signaling pathway regulates breast cancer cell migration by maintaining slug expression. Cancer Res 2009;69(24):9228–35 doi 10.1158/0008-5472.CAN-09-1950. [PubMed: 19920183]

41. Yoshino S, Hara T, Nakaoka HJ, Kanamori A, Murakami Y, Seiki M, et al. The ERK signaling target RNF126 regulates anoikis resistance in cancer cells by changing the mitochondrial metabolic flux. Cell Discov 2016;2:16019 doi 10.1038/celldisc.2016.19. [PubMed: 27462466]

Statement of Translational Significance

Effective predictive and therapeutic approaches to circumvent the potential impediments in the treatment of the more aggressive and metastatic form of luminal breast tumors, is yet to be developed. RAD51AP1-DYRK4 fusion could be the most frequently expressed tumor-specific fusion transcript reported in luminal breast tumors. This discovery sheds light on a new area of molecular pathobiology of these tumors, by revealing a new form of molecular events that may confer their aggressiveness and metastasis-prone behaviors. This study also suggests the potential of targeting the fusion-driven MEK signaling in the management of RAD51AP1-DYRK4 expressing luminal breast tumors.

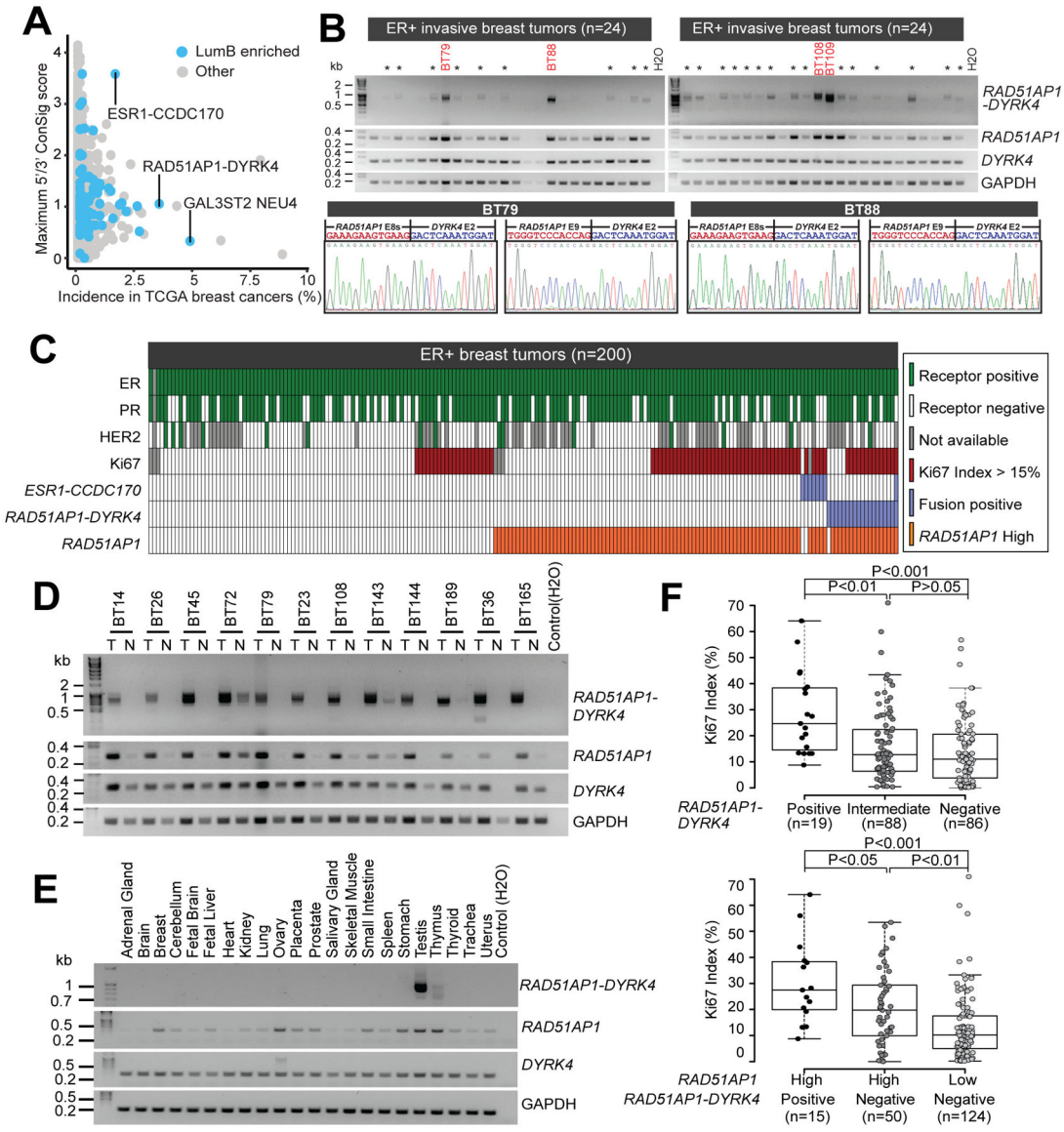

Figure 1. Discovery and validation of *RAD51AP1-DYRK4* as pathological chimerial transcript ectopically expressed in luminal B breast cancer.

(**A**) The chimerical transcripts identified in the TCGA breast cancer samples are classified by their enrichment in the luminal B breast cancer, and then prioritized by their ConSig scores and overall incidence. The preferential presence of the chimerical transcripts in luminal B tumors vs luminal A tumors was assessed by two-proportion Z-statistics. (**B**) RT-PCR validation of *RAD51AP1-DYRK4* in ER$^+$ breast cancer tissues using a forward primer in the first exon of *RAD51AP1* and a reverse primer in the second exon of *DYRK4.* Representative RT-PCR gel images are shown in the upper panel, and representative chromatograms of each *RAD51AP1-DYRK4* fusion variants are shown in the lower panel. *Weak *RAD51AP1-DYRK4* expression. (**C**) Heat map showing the receptor status, Ki67 index, *ESR1-CCDC170* or *RAD51AP1-DYRK4* status (strong positivity), and *wtRAD51AP1* overexpression in 200 ER+ breast cancer tissues. (**D**) RT-PCR analysis of *RAD51AP1-DYRK4* in paired tumor (T) and adjacent normal tissues (N) from 12 strong

positive cases reveals the tumor-specific expression of the *RAD51AP1-DYRK4* transcript. *WtRAD51AP1*, *wtDYRK4*, and *GAPDH* were used as controls. (**E**) Representative RT-PCR results of *RAD51AP1-DYRK4*, wt*RAD51AP1*, and wt*DYRK4* in normal human tissue panels. (**F**) Box plots comparing the Ki67 index for *RAD51AP1-DYRK4* strong positive, weak positive, and negative breast tumors (upper panel), or comparing *RAD51AP1-DYRK4* strong positive, RAD51AP1 high, and RAD51AP1 low fusion-negative tumors (lower panel). *P*-value was determined by t-test.

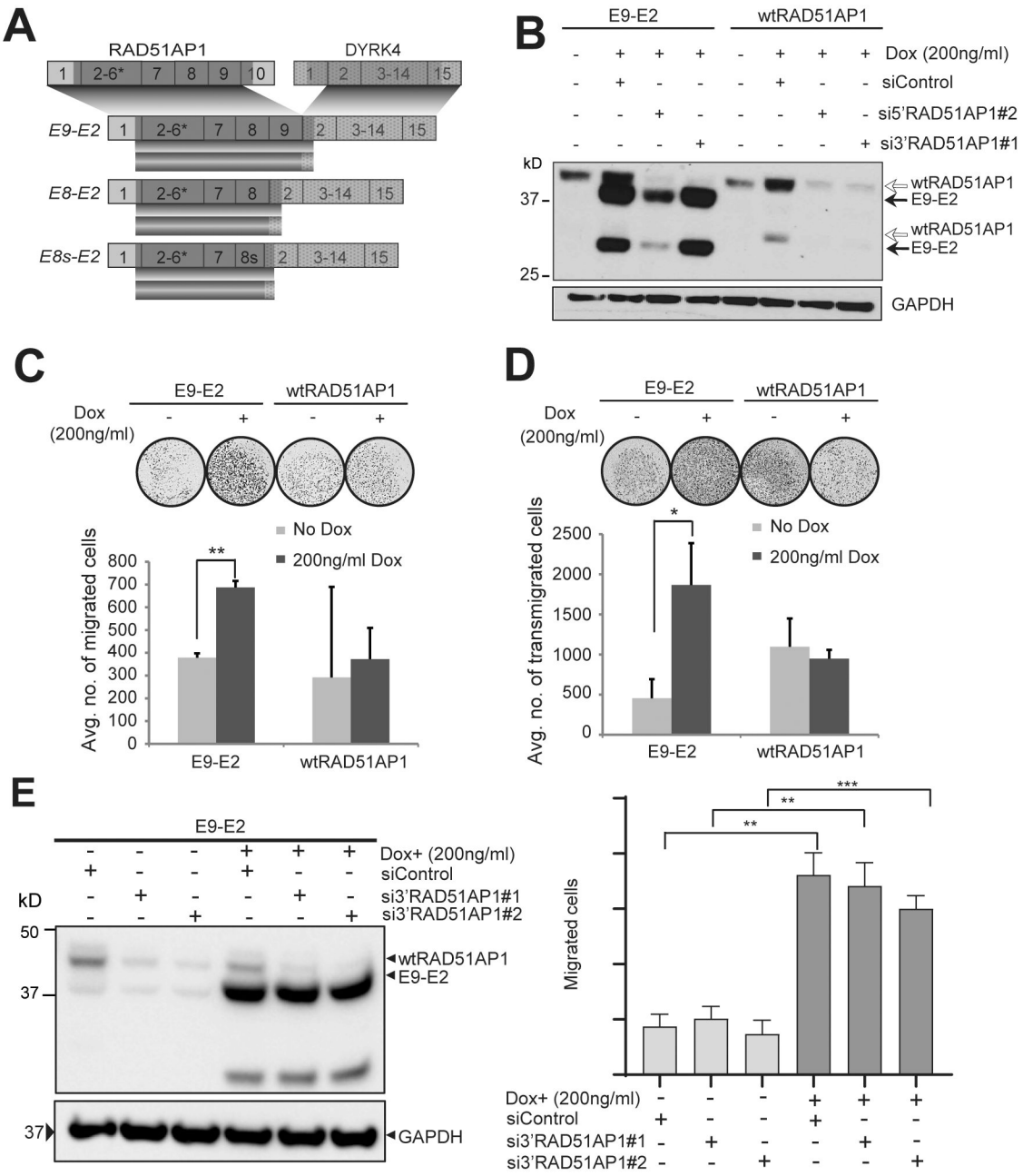

Figure 2. Characterization of protein product of RAD51AP1-DYRK4 and its oncogenic potential.

(**A**) Schematic of *RAD51AP1-DYRK4* fusion variants and their encoded proteins identified in breast cancer cell lines. ORFs are depicted in dark shades. (**B**) Immunoblot analysis of T47D cells inducibly expressing *RAD51AP1-DYRK4* (E9-E2 variant) or *wtRAD51AP1* using an anti-RAD51AP1 polyclonal antibody. To verify the identity of the fusion protein bands, the engineered T47D cells are transfected with 5'RAD51AP1 siRNA designed to knockdown both *RAD51AP1-DYRK4* and *wtRAD51AP1*, or the 3'RAD51AP1 siRNA designed to only inhibit the wtRAD51AP1. (**C**) Induction of *RAD51AP1-DYRK4* ectopic expression (E9-E2 variant) in T47D cells resulted in a significant increase in cell motility. T47D cells inducibly expressing *wtRAD51AP1* was used as control. (**D**) Ectopic expression

of *RAD51AP1-DYRK4* (E9-E2 variant) but not *wtRAD51AP1* resulted in a significant increase in transendothelial migration of T47D cells. The T47D cells inducibly expressing *E9-E2* or *wtRAD51AP1* were treated with doxycycline and allowed to migrate through a confluent monolayer of human umbilical vein endothelial cells (HUVECs). (**E**) Silencing of wtRAD51AP1 does not affect RAD51AP1-DYRK4 driven cell motility. Left, specific knockdown of wtRAD51AP1 using two siRNAs against its 3' region was verified by Western blotting. Cells are collected 48 hours following transfection with 10nM 3'RAD51AP1 siRNAs or control siRNA. Right, transwell migration assay following induced E9-E2 overexpression and silencing of wtRAD51AP1. NIH 3T3 cells and 20%FBS are used as chemoattractant. ($P<0.05$, *, $P<0.01$**, $P<0.001$***).

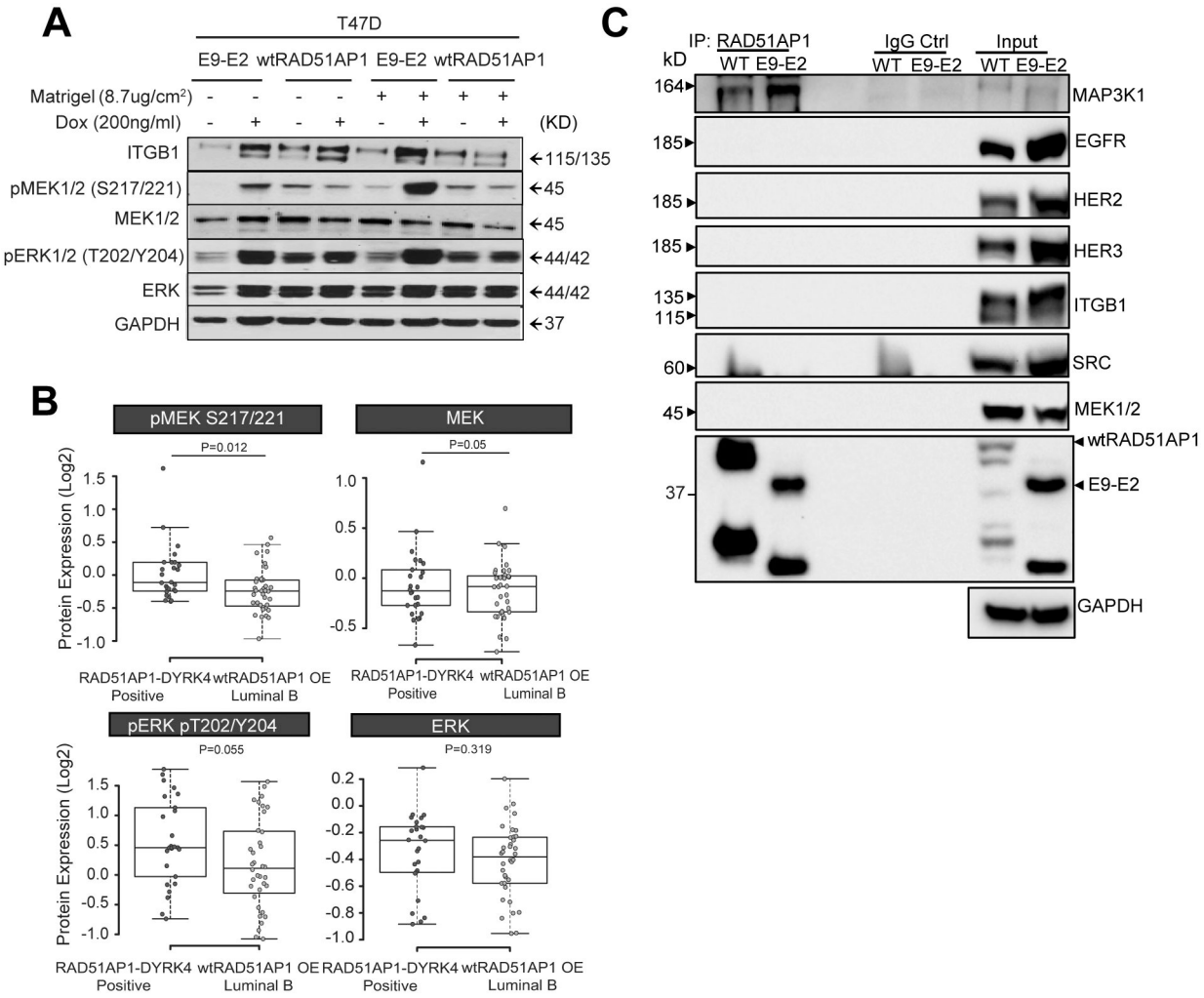

Figure 3. RAD51AP1-DYRK4 forms complex with MAP3K1 and activates MEK/ERK signaling.

(**A**) The impact of RAD51AP1-DYRK4 or wtRAD51AP1 overexpression on the cellular signaling of the respective engineered T47D cells in the presence or absence of Matrigel extracellular matrix. The expression of RAD51AP1-DYRK4 or wtRAD51AP1 is induced using doxycycline (Dox) for 1 week. (**B**) Increased activation of MEK/ERK in RAD51AP1-DYRK4 positive TCGA breast tumors (n=26) compared to fusion-negative LumB tumors overexpressing wtRAD51AP1 (n=36). The results are based on TCGA RPPA data. **(C)** Immuno-precipitation analysis of T47D cells ectopically expressing RAD51AP1-DYRK4 (E9-E2) or wtRAD51AP1. Lysates from T47D cells ectopically expressing E9-E2 or wtRAD51AP1 were immune-precipitated using anti-RAD51AP1 or control IgG antibodies. The IP fractions were immunoblotted with indicated antibodies. WT, wtRAD51AP1.

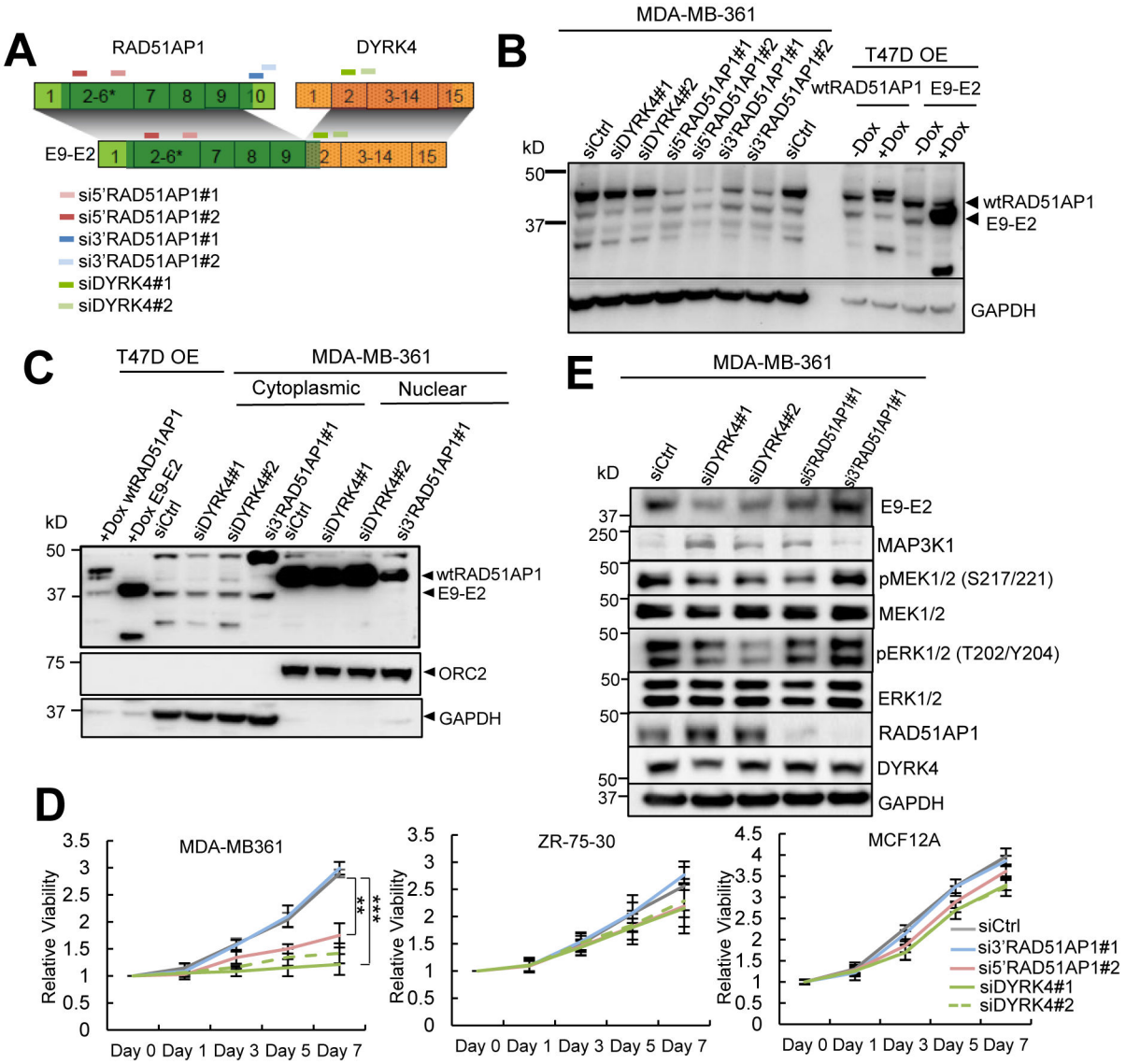

Figure 4. The function of endogenous RAD51AP1-DYRK4 protein expressed in the MDAMB361 luminal breast cancer cells.

(**A**) Schematic of two 5'RAD51AP1 siRNAs targeting both fusion and wtRAD51AP1, two 3'RAD51AP1 siRNAs specifically targeting wtRAD51AP1, and two DYRK4 siRNAs targeting both fusion and wtDYRK4. (**B**) Detecting endogenous RAD51AP1-DYRK4 protein through western blot analysis of MDAMB361 cells treated with control siRNA (siCtrl), DYRK4 siRNAs, 5'RAD51AP1 siRNAs, or 3'RAD51AP1 siRNAs, using a RAD51AP1 polyclonal antibody. T47D cells inducibly expressing E9-E2 fusion or wtRAD51AP1 are used as positive controls. (**C**) Detecting endogenous RAD51AP1-DYRK4 protein in the nuclear or cytoplasmic fractions of the MDAMB361 cells treated with different siRNAs, using the RAD51AP1 polyclonal antibody. (**D**) Viability of MDAMB361 cells following treatment with siRNAs against 5'RAD51AP1, 3'RAD51AP1, or DYRK4 (MTS assay). **p<0.01 (t-test). P values represent results of Student's T-test. **p<0.01, ***p<0.001 (compared to scrambled control siRNA at day 7). (**E**) The impact of silencing

endogenous RAD51AP1-DYRK4 on MAP3K1/MEK/ERK signaling in MDAMB361 fusion-positive cells treated with indicated siRNAs. The E9-E2 protein was detected using the fusion-specific customized polyclonal antibody.

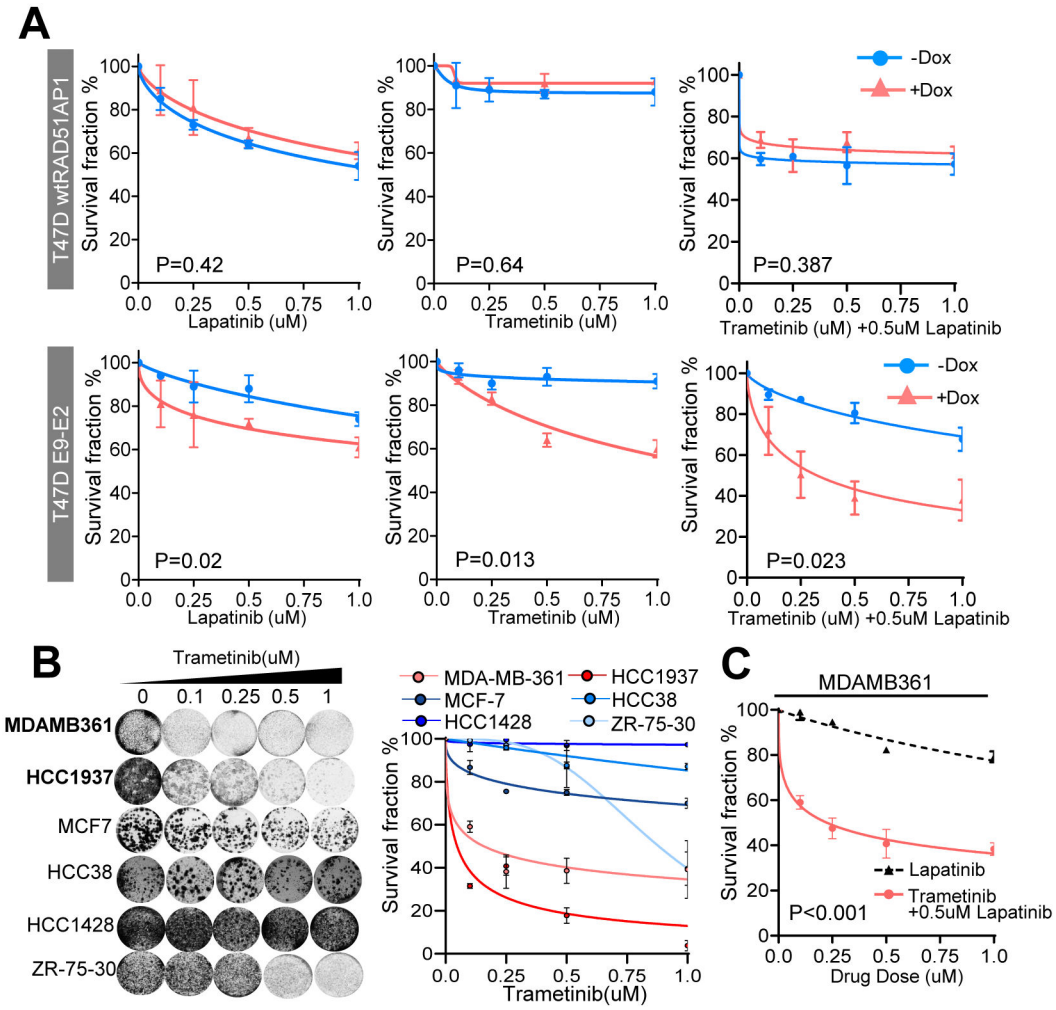

Figure 5. RAD51AP1-DYRK4 endows increased sensitivity to the MEK inhibitor Trametinib.

(**A**) T47D cells inducibly overexpressing E9-E2 but not wtRAD51AP1 exhibit significantly increased sensitivity to Trametinib treatment as shown by clonogenic assays. Lapatinib alone or in combination with Trametinib did not show additional therapeutic benefits. (**B**) The effect of trametinib treatment in a panel of breast cancer cell lines with (bold font) or without *RAD51AP1-DYRK4* overexpression (regular font) as shown by clonogenic assays. (**C**) MDAMB361 cells overexpressing endogenous RAD51AP1-DYRK4 exhibit lapatinib resistance but highly sensitive to concomitant trametinib and lapatinib treatment as shown by clonogenic assays. P<0.05, *, P<0.01**, P<0.001*** (Two-way Anova).

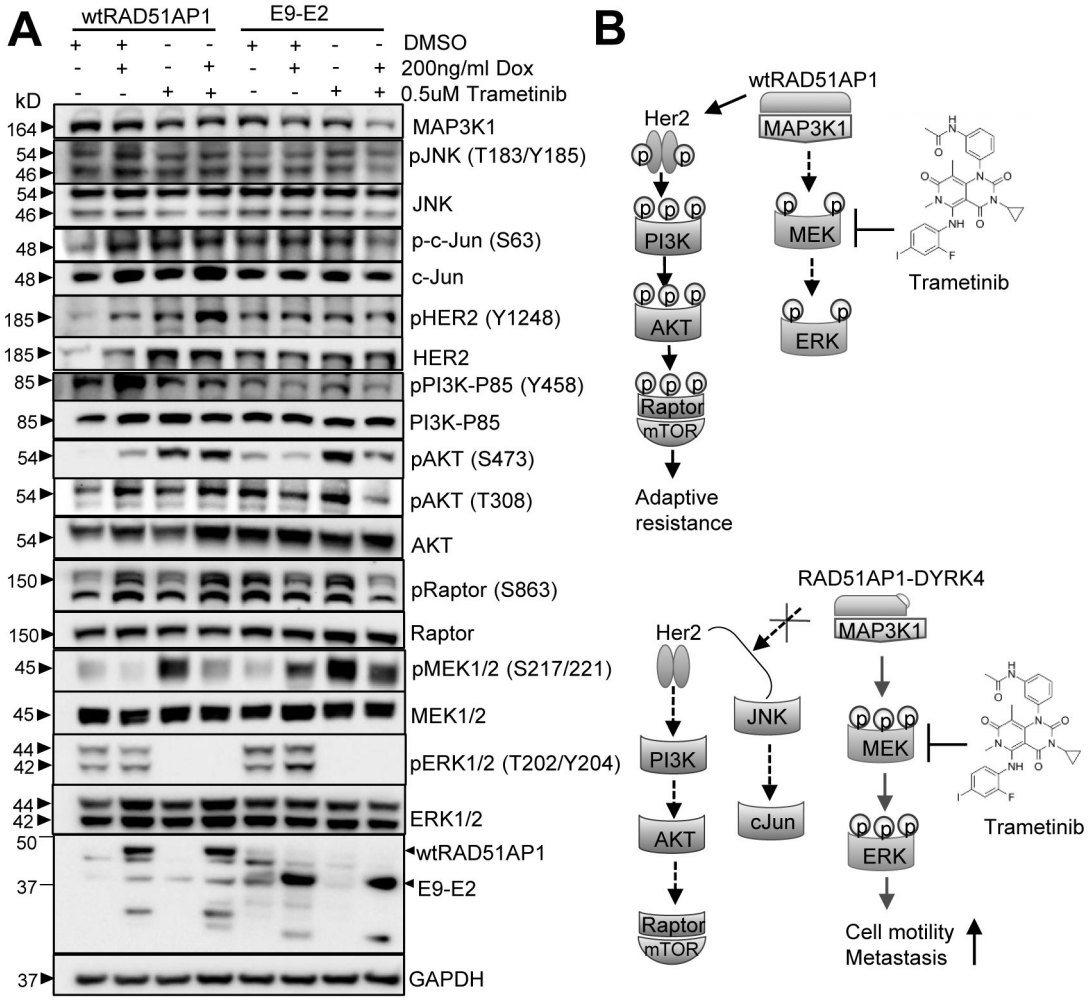

Figure 6. RAD51AP1-DYRK4 represses compensatory feedback loop following MEK inhibition.

(A) Western blot analysis of the engineered T47D cells inducibly overexpressing wtRAD51AP1 or E9E2 fusion harvested following trametinib or vehicle (DMSO) treatments. Cells were treated with doxycycline to induce wtRAD51AP1 or E9E2 expression for one week, and then treated with 0.5uM of MEK inhibitor (Trametinib) or vehicle (DMSO) for 24 hours. **(B)** A schematic of the mechanisms engaged by RAD51AP1-DYRK4 to endow increased aggressiveness and sensitivity to MEK inhibition. RAD51AP1-DYRK4 forms complex with MAP3K1 and endow increased motility and metastasis via activation of MEK/ERK signaling. In addition, RAD51AP1-DYRK4 appears to endow synthetic lethality to the MEK inhibitor Trametinib via attenuating compensatory HER2/PI3K/AKT and JNK/c-Jun signaling pathways. In contrast, wtRAD51AP1 overexpressing cancer cells show compensatory activation of the HER2/PI3K/AKT under MEK inhibition, leading to adaptive resistance to trametinib.